Synthesis of Core Functionalized Polymer Micelles and Shell Cross-Linked Nanoparticles

Alexander D. Ievins, Xiaofan Wang, Adam O. Moughton, Jared Skey, and Rachel K. O'Reilly*

The Melville Laboratory for Polymer Synthesis, Cambridge University, Lensfield Road, Cambridge CB2 1EW, U.K.

Received December 5, 2007; Revised Manuscript Received February 7, 2008

ABSTRACT: We present the synthesis of novel core reactive spherical polymeric micelles and nanoparticles using nitroxide mediated polymerization (NMP) techniques. These nanostructures have terpyridine functionality selectively located within their hydrophobic core domain and have been further modified by metal complexation (with Fe, Ru, and Cu) within this domain to afford novel metal functionalized polymer nanostructures. The hydrodynamic diameters (D_h) of these micelles and hybrid nanoparticles were determined by dynamic light scattering (DLS), and the dimensions of the nanoparticles were characterized using transmission electron microscopy (TEM) and confirmation of the complexation was achieved using UV–vis analysis. The reactivity of the Cu-tethered metal complex within the nanostructures was investigated and was found to be an active catalyst for the 1,3-dipolar cycloaddition "click" reaction of azido and alkynyl functionalized small molecules. This strategy provides a versatile synthetic route toward the selective incorporation of active sites within the core domain of a polymer nanoparticle.

Introduction

As a result of recent advances in controlled radical polymerization (CRP) techniques, control over polymeric chain length and functionality can now be achieved with considerable accuracy.[1–7] Amphiphilic diblock copolymers formed by such techniques may self-assemble in selective solvents, into various morphologies, depending on the volume weight fraction of the hydrophilic domain.[8–10] This versatile assembly technique allows for the investigation into a range of nanostructure morphologies such as spherical polymer micelles,[11–16] toroids,[17] helices,[18,19] rods,[20,21] disks,[22,23] fibers,[24,25] vesicles,[26–28] and tubes.[29,30] Over the past few decades, significant interest and effort have been invested in the development of functional nanostructures. Spherical polymer micelles and nanoparticles are perhaps the most exciting functional assemblies due to their potential application as delivery vehicles for therapeutics and imaging agents, as smart materials, and as functional nanoreactors.[31–36] Often this range of applications requires both robust stabilized structures and also the covalent attachment of functional molecules into selective domains of the nanoparticle scaffold.[36,37] Thus, the ability to tailor the chemical functionality of these various nanostructures is central in the development of their potential applications,[38,39] and as a result, there has been great recent interest in the development of methodologies for the cross-linking and functionalization of polymer micelles.

The stabilization of polymeric micelles is well established and can be achieved through covalent cross-linking, in either the core or shell domains, to afford stabilized amphiphilic nanoparticles with well-defined core–shell morphologies.[40–49] By limiting the cross-links to the polymer chain segments that compose the peripheral shell, shell cross-linked micelles or nanoparticles (often termed SCKs or SCLs) can be formed, which consist of a hydrophobic core domain and a cross-linked hydrophilic shell layer.[31,44,50] Cross-linking of the shell imparts stabilization yet has been demonstrated to retain the permeability of the shell layer, allowing for the diffusion of small molecules in and out of the nanostructure.[51,52] One disadvantage of this methodology is the requirement for relatively high dilution to avoid undesirable intermicellar cross-linking. To overcome this, Armes and co-workers have pioneered the synthesis and application of triblock copolymer systems which allow for cross-linking selectively through the inner shell layer to prevent intermicellar fusion, thereby enabling nanoparticle synthesis at higher and more commercially applicable concentrations.[53]

The selective functionalization of the hydrophobic core domains of polymeric micelles is an exciting area of research due to the potential application of the resulting materials as novel supported catalyst systems.[54] The covalent attachment of specific groups within the hydrophobic core, which can be protected from hydrolysis or degradation by the surrounding hydrophilic corona, allows for the selective reaction of hydrophobic reagents within this central domain in an overall hydrophilic or aqueous environment.[55,56] However, the functionalization of the core domain within polymeric micelles has received somewhat limited attention. A recent strategy that has successfully been employed is the synthesis of functionalized monomers, which can be incorporated selectively into the hydrophobic domain to allow for the placement of reactive handles throughout the core region. The functionality embedded and dispersed throughout the core of polymeric micelles has been demonstrated to be available and reactive toward further chemical modification.[52]

An alternative approach which has been recently reported by McQuade uses a urea polymeric shell for catalysis and affords soluble catalytic polymeric microcapsules which are created via sequestration of latently functionalized polymers to allow for further capsule modification.[57] In this work the authors report that single site active catalysts could be generated inside these polymeric microcapsules and that they demonstrated higher activity than resin-supported catalysts in a range of catalytic reactions such as DMAP acylation and oxidation reactions using TEMPO.

The application of terpyridine functionalized polymers as reactive copolymers has been extensively studied by Schubert and co-workers.[58–61] They have elegantly demonstrated the application of metal–ligand-based complexation interactions based on terpyridine with a range of metal centers (such as Ru, Fe, Cu, Ni, and Zn)[62,63] for the assembly of polymers and micelles.[64–67] Tew and co-workers have also explored the

* Corresponding author. E-mail: rko20@cam.ac.uk.

10.1021/ma702702j CCC: $40.75
Published on Web 04/01/2008

terpyridine functionality as an important assembly unit using a novel methacrylate based terpyridine monomer which they polymerized using free radical techniques. They also reported the synthesis of copolymers with varying degrees of functional group incorporation for utilization in metal–ligand supramolecular association to form novel cross-linked networks.[68] In recent papers they have also reported using postpolymerization functionalization strategies and a controlled radical polymerization route for the synthesis of well-defined and tunable terpyridine functionalized polymers.[69–71]

In this paper the synthesis of amphiphilic copolymers in which the hydrophobic domain is selectively and tailorably functionalized with terpyridine groups is reported using nitroxide mediated polymerization (NMP) and established deprotection chemistries. The self-assembly, using solution techniques, of these functional blocks into core functionalized micelles is reported as is their subsequent stabilization throughout the shell layer and metal complexation. The application of these spherical robust micellar supports, which have been selectively complexed with Cu(I) in their core domain was investigated for Click cycloaddition catalysis.[72–74] In this initial work we highlight the potential of this strategy toward the synthesis of more complex functional and catalytically active phase-separated nanoreactors.

Experimental Section

Measurements. Hydrodynamic diameters (D_h), size distributions, and zeta potential (ζ) for the micelles and nanoparticles in aqueous solutions were determined by dynamic light scattering (DLS). The DLS instrumentation consisted of a Malvern Zetasizer Nano ZS instrument operating at 25 °C with a 635 nm laser module. Measurements were made at a detection angle of 173° (backscattering), and Malvern DTS 4.00 software was utilized to analyze the data. All determinations were made in triplicate (with 12 runs per record).

Transmission electron microscopy samples were diluted with a 1% phosphotungstic acid (PTA) stain (1:1). Copper/carbon grids were prepared by argon plasma treatment to increase the surface hydrophilicity. Micrographs were collected at magnifications varying from 42K to 130K and calibrated using an internal graticule. Histograms of number-average particle diameters (D_{av}) and standard deviations were generated from the analysis of a minimum of 150 particles from at least three different micrographs.

Nuclear magnetic resonance (^{1}H and ^{13}C) was performed on a Bruker AVANCE 400 or 500 MHz FT-NMR spectrometer using deuterated solvents. Gel permeation chromatography (GPC) data for all the polymers were obtained in THF (Shimadzu UFLC autosampler with Polymer Laboratories gel 5 μm Mixed C column) at room temperature with linear poly(methyl methacrylate) (PMMA) standards at a flow rate of 1 mL/min. The modulated differential scanning calorimetry (DSC) measurements were performed with a TA Instruments DSC 2920 and with a ramp rate of 4 deg/min. The glass-transition temperatures (T_g) were taken as the midpoint of the inflection tangent, upon the third heating scan. Infrared spectra (IR) were obtained on a Perkin-Elmer Spectrum 100 ATR FT-IR spectrometer. Fluorescence spectroscopy data were acquired on a Varian Cary Eclipse fluorescence spectrophotometer, each sample was excited at $\lambda_{ex} = 496$ nm, and the fluorescence emission spectra in the range 500–700 nm were recorded.

Materials. *tert*-Butyl acrylate (*t*BuA) and styrene (St) were purified by vacuum distillation from CaH_2 and then stored at –15 °C. Dichloromethane (CH_2Cl_2) was dried by prolonged refluxing over calcium hydride. All other materials were used as received from Sigma-Aldrich Co. Supor 25 mm 0.1 μm Spectra/Por membrane tubes (Spectrum Medical Industries Inc., Laguna Hills, CA) were used for dialysis. The following materials were synthesized according to literature methods: 2,2,5-trimethyl-3-(1-phenylethoxy)-4-phenyl-3-azahexane,[75] 2,2,5-trimethyl-4-phenyl-3-azahexane 3-nitroxide,[75] 2,6-bis(pyrid-2-yl)-4-pyridone,[76] CuBr-$(PPh_3)_3$,[77] and 3-azidocoumarin.[78]

Synthesis. *Synthesis of 4′-(4-Vinylbenzyloxy)-2,2′:6′,2″-terpyridine,* ***1***. The functional monomer was synthesized following a

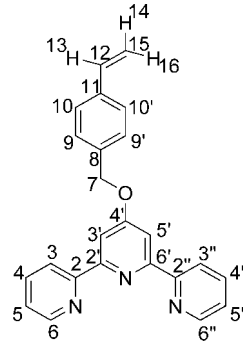

modified literature procedure.[60,79] To a suspension of 2,6-bis(pyrid-2-yl)-4-pyridone (2.5 g, 10.0 mmol) and K_2CO_3 (4.9 g, 35.5 mmol) in anhydrous DMF (30 mL) at 50 °C under N_2, a solution of 4-vinylbenzyl chloride (2.28 g, 15.0 mmol) in anhydrous DMF (20 mL) was added dropwise. Stirring was continued at 50 °C for 2 days, after which the mixture was poured into 250 mL of cold, deionized water (250 mL) and extracted with CH_2Cl_2 (5 × 150 mL) and washed with brine (5 × 150 mL). The combined organic layers were dried (Na_2SO_4), filtered, and evaporated in vacuo. The crude product was purified by column chromatography (neutral alumina, CH_2Cl_2 + 3% CH_3OH, $R_f = 0.5$) to yield an off-white solid (2.27 g, 63%). ^{1}H NMR (400 MHz, $CDCl_3$), δ_H: 8.68 (dd, 2H, $J = 4.0$, 2.0 Hz, $H_{6,6''}$), 8.61 (dd, 2H, $J = 7.6$, 2.4 Hz, $H_{3,3''}$), 8.12 (s, 2H, $H_{3',5'}$), 7.84 (ddd, 2H, $J = 7.6$, 7.2, 1.6 Hz, $H_{4,4''}$), 7.44 (s, 4H, $H_{9,9',10,10'}$), 7.32 (ddd, 2H, $J = 1.2$, 4.8, 7.2 Hz, $H_{5,5''}$), 6.72 (dd, 1H, $J = 17.6$, 10.8 Hz, H_{13}), 5.76 (dd, 1H, $J = 17.6$, 0.8 Hz, H_{16}), 5.31 (s, 2H, H_7), 5.26 (dd, 1H, $J = 10.8$, 0.8 Hz, H_{14}). ^{13}C NMR (400 MHz, $CDCl_3$), δ_C: 166.9 ($C_{4'}$), 157.2 ($C_{2',6'}$), 156.1 ($C_{2,2''}$), 149.0 ($C_{6,6''}$), 136.8 (C_8), 136.5 ($C_{4,4''}$), 136.4 (C_{12}), 135.6 (C_{11}), 127.7 ($C_{9,9'}$), 126.4 ($C_{10,10'}$), 123.8 ($C_{3,3''}$), 121.3 ($C_{5,5''}$), 114.2 (C_{15}), 107.6 ($C_{3',5'}$), 69.7 (C_7). IR, ν (cm^{-1}): 3089, 3053, 2926, 1629, 1600, 1581, 1560, 1514, 1467, 1453, 1443, 1418, 1406, 1351, 1278, 1253, 1217, 1191, 1118, 1099, 1092, 1064, 1014, 998, 989, 925, 875, 864, 850, 829, 802, 789, 742, 728, 695, 658. Melting point: 121 °C. Elemental analysis: theoretical %: C 78.88, H 5.24, N 11.50; experimental %: C 78.62, H 5.27, N 11.51.

General Polymerization Conditions for the Synthesis of Polymers ***2***–***5***. A mixture of the alkoxyamine (2,2,5-trimethyl-3-(1-phenylethoxy)-4-phenyl-3-azahexane) (15.6 mg, 0.048 mmol), styrene (1.1 mL, 1.0 g, 9.6 mmol), and **1** (in varying molar ratios to styrene) was degassed by three freeze/pump/thaw cycles, sealed under argon, and heated at 125 °C for varying amounts of time. The viscous reaction mixture was then dissolved in THF (5 mL) and precipitated three times into MeOH (200 mL) at 4 °C. The resulting white solid was dried under vacuum at 40 °C overnight.

2: Ratio of St:**1**:initiator = 200:7:1. (0.65 g, 65% yield, 3.7% relative incorporation of **1**). ^{1}H NMR (500 MHz, $CDCl_3$), δ_H: 8.7–8.6 (br d, $4H_{terpy}$), 8.2–8.1 (br s, $2H_{terpy}$), 7.9–7.8 (br s, $2H_{terpy}$), 7.5–7.4 (br s, $4H_{terpy}$), 7.3–6.3 (br m, aromatic signals from both monomers and end groups), 5.3–5.2 (br s, $2H_{terpy\ backbone}$), 2.2–1.2 (br m, backbone and end group signals). M_n(NMR) = 8 700, M_n(GPC, THF) = 8 300, PDI = 1.17. IR, ν (cm^{-1}): 3059, 3026, 2921, 2849, 1985, 1940, 1601, 1582, 1564, 1492, 1452, 1407, 1354, 1196, 1154, 1091, 1067, 1028, 906, 842, 795, 756, 703, 660. DSC: T_g 105 °C.

3: As described for **2**, except ratio of St:**1**:initiator = 200:10:1 (0.51 g, 51% yield, 5.2% relative incorporation of **1**), M_n(NMR) = 17 100, M_n(GPC, THF) = 16 100, PDI =1.21; DSC: T_g 107 °C.

4: As described for **2**, except ratio of St:**1**:initiator = 200:20:1 and 1 mL of DMF was added (0.41 g, 41% yield, 11.8% relative

incorporation of **1**), M_n(NMR) = 15 400, M_n(GPC, THF) = 14 000, PDI = 1.26; DSC: T_g 111 °C.

5: As described for **2**, except ratio of St:**1**:initiator = 200:50:1 and 1 mL of DMF was added (0.45 g, 45% yield, 29.4% relative incorporation of **1**), M_n(NMR) = 18 600, M_n(GPC, THF) = 13 800, PDI = 1.34; DSC: T_g 118 °C.

*Preparation of PtBuA$_n$ Macroinitiator, **6***. A mixture of alkoxyamine initiator (0.065 g, 0.18 mmol) and free nitroxide (0.002 g, 0.01 mmol) was dissolved in *tert*-butyl acrylate (4.62 g, 36.07 mmol), and the solution was sealed in a glass ampule equipped with a stirrer bar, degassed, and stored under N_2. The vessel was then heated to 125 °C with stirring for 48 h. After cooling, THF (15 mL) was added to dissolve the product, and the solution added to a large excess of methanol (300 mL), ice (15 cm^3), and dry ice, with stirring. The solvent was removed in vacuo, further THF (20 mL) added, the solution dried ($MgSO_4$), and the solvent removed in vacuo and reprecipitated as described above. The product was further dried under high vacuum overnight at 25 °C and collected as an amorphous white solid (2.59 g, 43%). ^{1}H NMR (500 MHz, $CDCl_3$), δ_H: 7.4–7.0 (br m, chain-end phenyl H), 1.5–1.3 (br m, aliphatic backbone, *tert*-butyl groups and chain-end signals). M_n(NMR) = 17 700, M_n(GPC, THF) = 17 400, PDI = 1.18. IR, ν (cm^{-1}): 3306, 2977, 1726, 1480, 1447, 1392, 1366, 1255, 1142, 845, 752. DSC: T_g 47 °C.

*Preparation of Poly(tert-butyl acrylate)-b-(polystyrene-co-poly(4′-(4-vinylbenzyloxy)-2,2′:6′,2″-terpyridine)), **7***. A mixture of styrene (0.566 g, 5.43 mmol), 4′-(4-vinylbenzyloxy)-2,2′:6′,2″-terpyridine, **1** (0.105 g, 0.29 mmol, 5% relative to styrene), and the poly(*tert*-butyl acrylate) macroinitiator, **6** (0.500 g, 0.03 mmol), was sealed in a glass ampule equipped with a stirrer bar, degassed, and stored under N_2. The vessel was then heated to 125 °C for 16 h. After cooling, THF (15 mL) was added to dissolve the product, and the solution was added to a large excess of methanol (300 mL) and dry ice, then filtered, and repeated twice. The product was further dried in vacuo overnight at 25 °C and collected as an amorphous white solid (0.73 g, 62%). ^{1}H NMR (500 MHz, $CDCl_3$), δ_H: 8.7–8.5 (br m, 4H$_{terpy}$), 8.2–7.9 (br m, 2H$_{terpy}$), 7.9–7.7 (br m, 2H$_{terpy}$), 7.3–7.2 (br m, 2H$_{terpy}$), 7.2–6.2 (br m, aromatic signals from both monomers and end groups), 5.3–4.9 (br s, 2H$_{terpy\ backbone}$), 2.4–1.0 (br m, *tert*-butyl group and polymer backbone). M_n(NMR) = 29 400 and 6.3 mol % terpyridine-functionalized monomer incorporation, M_n(GPC, THF) = 26 800, PDI = 1.23. IR, ν (cm^{-1}): 2978, 2824, 1726, 1601, 1582, 1564, 1493, 1452, 1393, 1367, 1255, 1145, 845, 795, 755, 697. DSC: $T_{g(PtBuA)}$ 46 °C, $T_{g(PS\text{-}co\text{-}PSTerpy)}$ 111 °C.

*Preparation of Poly(acrylic acid)-b-(polystyrene-co-poly(4′-(4-vinylbenzyloxy)-2,2′:6′,2″-terpyridine)), **8***. Poly(*tert*-butyl acrylate)-*b*-(polystyrene-*co*-poly(4′-(4-vinylbenzyloxy)-2,2′:6′,2″-terpyridine)) (0.250 g, 0.0084 mmol, 1.17 mmol of *tert*-butyl ester groups) was added to anhydrous CH_2Cl_2 (10 mL) at 0 °C and allowed to stir for 1 h. A 10-fold molar excess (relative to *tert*-butyl acrylate side-chain units) of trifluoroacetic acid (1.27 g, 11.17 mmol) was added dropwise to the stirred solution, which was then allowed to warm to RT. Stirring was continued for 1 day, after which air was gently blown over the solution to drive off CH_2Cl_2 and excess trifluoroacetic acid. Then 10 mL of each of THF and water were added, and the solution was then exhaustively dialyzed into distilled water with presoaked dialysis membrane tubes (MWCO ca. 3.5 kDa) and then freeze-dried. The product was collected as a white fluffy solid (0.13 g, 72%). ^{1}H NMR (500 MHz, d_6-DMSO), δ_H: 13.1–12.3 (br s, OH), 8.7–8.5 (br m, 4H$_{terpy}$), 8.2–7.9 (br m, 2H$_{terpy}$), 7.9–7.7 (br m, 2H$_{terpy}$), 7.3–7.2 (br m, 2H$_{terpy}$), 7.2–6.1 (br m, aromatic signals from both monomers and end groups), 5.3–4.9 (br m, 2H$_{terpy\ backbone}$), 2.4–1.0 (br m and polymer backbone). M_n(NMR) = 21 800 and 6.3 mol % terpyridine-functionalized monomer incorporation. IR, ν (cm^{-1}): 3026, 2925, 1706, 1601, 1582, 1565, 1493, 1452, 1408, 1248, 1168, 1028, 795, 758, 698. DSC: $T_{g(PAA)}$ 132 °C, $T_{g(PS\text{-}co\text{-}PSTerpy)}$ 109 °C.

*Preparation of Micelles from Poly(acrylic acid)-b-(polystyrene-co-poly(4′-(4-vinylbenzyloxy)-2,2′:6′,2″-terpyridine)), **9***. A round-bottom flask equipped with a stirrer bar was charged with PAA$_n$-*b*-(PS-*co*-PSTerpy)$_m$, **8** (M_n(NMR) = 21 800 g/mol; 0.070 g, 0.0032 mmol), and THF (70 mL) was added, and the solution was allowed to stir at room temperature for 30 min to ensure the mixture was homogeneous. Deionized water (70 mL) was added via a metering pump at the rate of 15 mL/h. After all the water had been added, the bluish micelle solution was transferred to presoaked dialysis membrane tubes (MWCO ca. 3.5 kDa) and dialyzed against deionized water for 4 days. The final volume of **9** was 180 mL, affording a polymer concentration of ca. 0.38 mg/mL. D_h(DLS) = 67 ± 3 nm; ζ: −49 ± 1 mV; D_{av}(TEM): 61 ± 5 nm. IR, ν (cm^{-1}): 3060, 3026, 2924, 1707, 1602, 1583, 1560, 1493, 1452, 1359, 1231, 1179, 1120, 1065, 1028, 907, 861, 796, 756, 679; DSC: $T_{g(PAA)}$ = 136 °C, $T_{g(PS\text{-}co\text{-}PSTerpy)}$ = 105 °C.

*Preparation of Nanoparticles by Covalent Cross-Linking 50% of Acrylic Acid Residues Selectively in the Micelle Shell Layer, **10***. To a stirred solution of micelle **9** (50 mL, 0.38 mg/mL, 0.13 mmol of acrylic acid) in a round-bottom flask equipped with a stirrer bar was added, dropwise over 10 min, a solution of 2,2′-(ethylenedioxy)bis(ethylamine) (0.005 g, 0.032 mmol) in deionized water (2 mL). The solution was allowed to stir for 2 h at RT. To this reaction mixture was added dropwise via a metering pump at the rate of 15 mL/h a solution of 1-[3′-(dimethylamino)propyl]-3-ethylcarbodiimide methiodide (0.019 g, 0.064 mmol) dissolved in deionized water (5 mL). The reaction mixture was allowed to stir overnight at RT and was then transferred to presoaked dialysis membrane tubes (MWCO ca. 6–8 kDa) and dialyzed against deionized water for 4 days to remove small molecule contaminants. The final volume of **10** was ca. 60 mL, affording a polymer concentration of ca. 0.32 mg/mL. D_h(DLS) = 58 ± 2 nm; ζ: −21 ± 1 mV; D_{av}(TEM): 52 ± 4 nm. IR, ν (cm^{-1}): 3354, 3061, 3026, 2925, 1707, 1641, 1602, 1585, 1560, 1493, 1452, 1391, 1353, 1261, 1092, 1028, 965, 909, 796, 748, 698, 659, 654. DSC: $T_{g(PS\text{-}co\text{-}PSTerpy)}$ = 107 °C.

*Metal Complexation of the Terpyridine Ligands within the Nanoparticle Core, **11** and **12***. **11**: Ruthenium(III) chloride hexahydrate (ca. 25 mg) was added to a stirred solution of the nanoparticles (5 mL, 0.32 mg/mL) and THF (0.5 mL) to solubilize the core and then heated to 45 °C overnight, after which the solution was dialyzed into nanopure water for the removal of excess metal (MWCO ca. 6–8 kDa) and then filtered using a 0.45 μm Teflon filter for the removal of insoluble aggregates. A brown solution of **11** resulted. D_h(DLS) = 62 ± 3 nm; ζ: −25 ± 2 mV; D_{av}(TEM): 58 ± 4 nm. IR, ν (cm^{-1}): 3355, 3061, 3023, 2925, 1639, 1560, 1493, 1453 1391, 1359, 1261, 1091, 1028, 965, 909, 799, 748, 698, 656. UV/vis, λ (nm): 390 (MLCT band).

12: Iron(III) chloride hexahydrate (ca. 25 mg) was added to a stirred solution of the nanoparticles (5 mL, 0.32 mg/mL) and THF (0.5 mL) to solubilize the core, then heated to 45 °C, and stirred at this temperature overnight, after which the solution was dialyzed into nanopure water for the removal of excess metal (MWCO ca. 6–8 kDa) and then filtered using a 0.45 μm Teflon filter for the removal of insoluble aggregates. A pale orange solution of **12** resulted. D_h(DLS) = 55 ± 5 nm; ζ: −28 ± 3 mV. IR, ν (cm^{-1}): 3346, 3058, 3031, 2925, 1707, 1641, 1616, 1573, 1483, 1452, 1393, 1353, 1263, 1092, 1027, 965, 909, 752, 698, 661, 654. UV/vis, λ (nm): 550 (MLCT band).

*Copper Catalyzed Click Reaction within the Nanoparticle Core Using Terpyridine Functionalized Nanoparticle and Cu(I) Salt, **13***. The hydrophobic core of nanoparticle **10** (10 mL, 0.32 mg/mL) was first swollen by dialysis (MWCO ca. 6–8 kDa) into a solution of DMF and water (1:10 v/v). Then $CuBr(PPh_3)_3$ (ca. 5 mg) was added to a stirred solution of the nanoparticles and allowed to stir for 1 h. A UV–vis spectrum of **13** was taken, and a characteristic MLCT band for the formation of a copper−terpyridine complex was observed at 330 nm. D_h(DLS) = 82 ± 5 nm; D_{av}(TEM): 63 ± 5 nm. Then 3-azidocoumarin (ca. 10 mg) and ethynylbenzene (ca. 10 mg) in DMF (0.5 mL) were added slowly to stirred solution of swollen nanoparticle **13**. After 4 h an aliquot was removed and analyzed by fluorescent analysis. Fluorescence, λ (nm): ca. 545 nm, D_h(DLS) = 84 ± 4 nm. The control reactions were performed with a nonfunctionalized swollen PAA$_{130}$-*b*-PS$_{100}$ nanoparticle (D_h(DLS) = 76 ± 4 nm and D_{av}(TEM) = 60 ± 6

Scheme 1. (a) Synthesis of Monomer 1 and (b) Conditions for the Copolymerization of 1 and Styrene via NMP

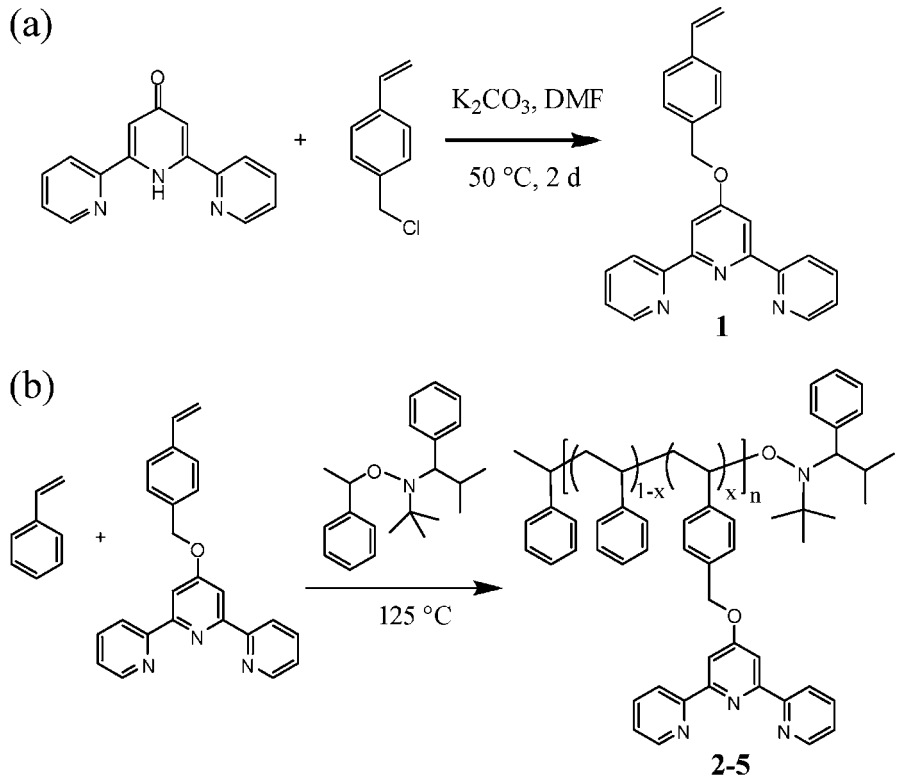

nm) prepared in a similar manner; no fluorescence was observed in the region 500–400 nm after reaction with the Cu(I), azido-coumarin, and alkynyl reagents.

Results and Discussion

Synthesis and Copolymerization of Novel Terpyridine Functional Monomer. Initial work focused on the synthesis of a styrenic based terpyridine monomer, **1** (Scheme 1a). Recently, Schubert and co-workers have reported the synthesis of **1** and a number of related styrene derivatized monomers;[79] however, the polymerization of this monomer has yet to be reported. Using a similar synthetic strategy, to that reported by Schubert, monomer **1** was synthesized in good yield from commercially available chloromethylstyrene and terpyridine−pyridone (which was readily afforded in two steps from ethyl picolinate as reported by Schubert).[76] Monomer **1** was isolated as an off-white solid and characterized by ^{1}H NMR, ^{13}C NMR, and IR spectroscopies and CHN microanalysis.

The copolymerization of monomer **1** with styrene was explored by nitroxide mediated polymerization (NMP) using Hawker's universal initiator (Scheme 1b).[75] By selectively altering the ratio of functional styrene (**1**) and styrene, this allowed access to a range of polymers which contained varying degrees (from 3.7% to 29.4%) of terpyridine functionality located along their side chain. The degree of incorporation of the functional monomer could be very easily determined by examination of the extended ^{1}H NMR spectrum of the resultant polymer and comparison of the signals attributable to the terpyridine moiety at ca. 8.6, 8.0, and 7.6 ppm, which correspond to 4H, 2H, and 2H, respectively, with those for the aromatic signals for the unfunctionalized polystyrene polymer. The presence of the terpyridine moiety was also confirmed by IR analysis with the characteristic signals at ca. 1600, 1582, and 1561 cm^{-1} clearly visible in the spectrum.

It has been reported in the literature that column affinity issues are often observed in the GPC analysis of terpyridine functional monomers which can lead to inaccurate molecular weight data.[65]

Table 1. Data for the Copolymerization of 1 and Styrene Using NMP at 125 °C (in All Reactions Styrene:Alkoxyamine Ratio Is 200:1)

polymer	initial mol % of **1**	time (h)	conv (%)	M_n (NMR)	M_n (GPC)	M_w/M_n	final mol % of **1**[a]
2	3.6	16	78	16 800	16 400	1.17	3.7
3	4.5	16	68	17 100	16 100	1.21	5.2
4[b]	9.0	16	47	15 400	14 000	1.26	11.8
5[b]	25.0	16	43	18 600	13 800	1.34	29.4

[a] As determined by extended ^{1}H NMR analysis of the worked up copolymer. [b] Polymerization was performed with 1 equiv of DMF (relative to the monomer).

As a result of this, NMR spectroscopy and the relative integration of the end-group signals (α-H at the nitroxide chain end at ca. 3.3 ppm) and the polymer backbone signals were utilized to determine the molecular weight of the resultant functional polymer. The kinetics of the copolymerization were determined using the conditions described for polymer **3**, and a plot of $\ln[M]_0/[M]_t$ was linear over time ($k_p = 0.123$ s^{-1}), indicating a controlled radical polymerization with a constant concentration of radicals throughout the polymerization; thus, no detectable termination is occurring during the polymerization. It was found that the introduction of a small amount of monomer **1** (ca. 5%) did not significantly alter the kinetics of the polymerization compared to those performed under identical conditions with just styrene (compared to the data from ref 75). However, it is clear from Table 1 that the incorporation of the functional terpyridine monomer did lead to a broadening of the polydispersity index relative to those obtained by Hawker in the NMP of styrene (ca. 1.1).[75]

Terpyridine Functionalized Amphiphilic Block Copolymer Formation. The goal of this work was to synthesize amphiphilic block copolymers which contained reactive and available terpyridine functionality within the hydrophobic segment and then investigate their assembly into spherical nanostructures and subsequent activity in catalysis. For the

Scheme 2. Synthesis, Using NMP, of a *tert*-Butyl Acrylate Block (6) Followed by Chain Extension To Form a Block Copolymer in Which the Styrenic Domain Contains a Specific Incorporation of Terpyridine Functionality (7), Followed by Formation of an Amphiphilic Diblock Copolymer with Terpyridine Functionality Embedded within the Hydrophobic Segment, 8

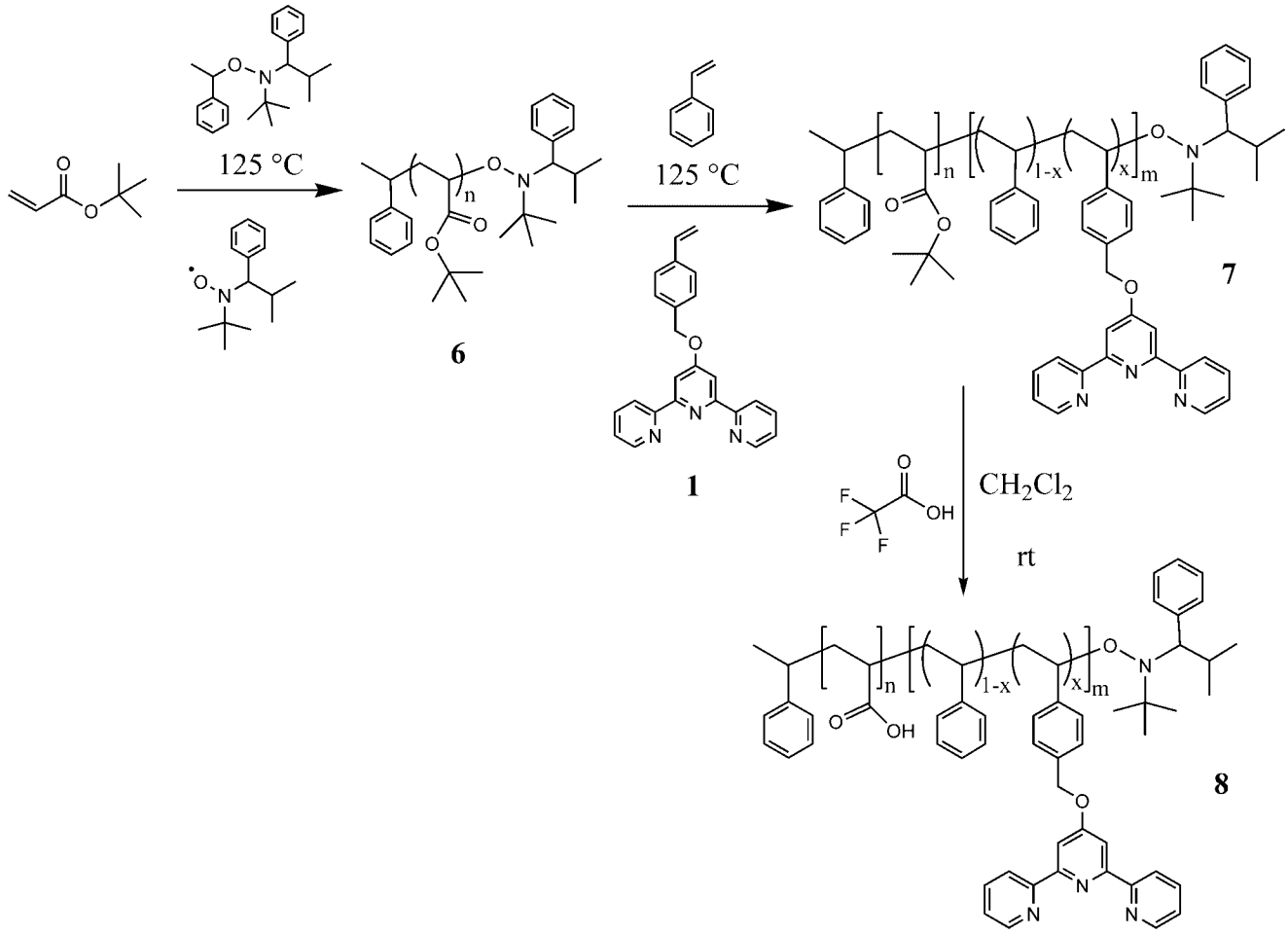

synthesis of the amphiphilic block copolymer a strategy was employed which involved the synthesis of a *tert*-butyl acrylate macroinitiator followed by chain extension with styrene and a predetermined ratio of functional styrenic monomer (**1**) to form a diblock in which the acrylate esters could be deprotected to afford carboxylic acid functionalities. Using previously established experimental conditions, the acrylate macroinitiator (**6**) was synthesized (Scheme 2) and characterized fully using ^{1}H NMR, GPC, and IR spectroscopy (M_n(NMR) = 17 700, M_n(GPC) = 15 400; M_w/M_n = 1.18).[75] Using the information previously obtained in the copolymerizations of **1** and styrene, an acrylate-*b*-functionalized styrene-*co*-styrene diblock copolymer, **7**, was afforded with excellent control by the chain extension of macroinitiator **6**, using the conditions outlined in Scheme 2 (**7**: M_n(NMR) = 29 400, M_n(GPC) = 26 800; M_w/M_n = 1.23). This block copolymer was found, by analysis of the ^{1}H NMR spectrum, to contain 6.3% incorporation of the terpyridine functionality throughout the styrenic domain. The conversion of block copolymer **7** to the amphiphilic poly(acrylic acid) derivative, **8**, was performed using established and high yielding deprotection chemistries, using trifluoroacetic acid as described previously by Wooley (Scheme 2).[80] This conversion of the ester groups to carboxylic acid functionality was

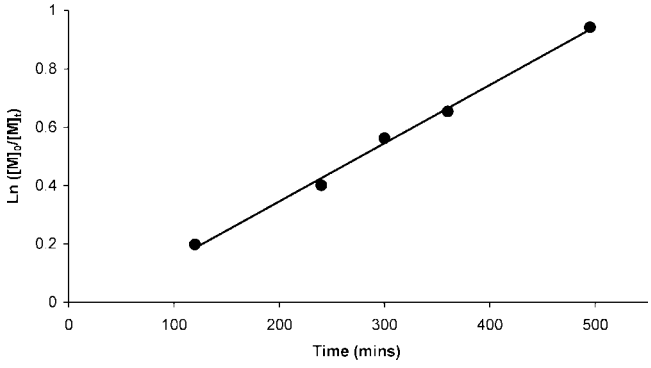

Figure 1. Plot of $[M]_0/[M]_t$ vs time for the copolymerization of **1** and styrene, using alkoxylamine initiator (ratio 9:200:1) at 125 °C using conditions as described in Table 1.

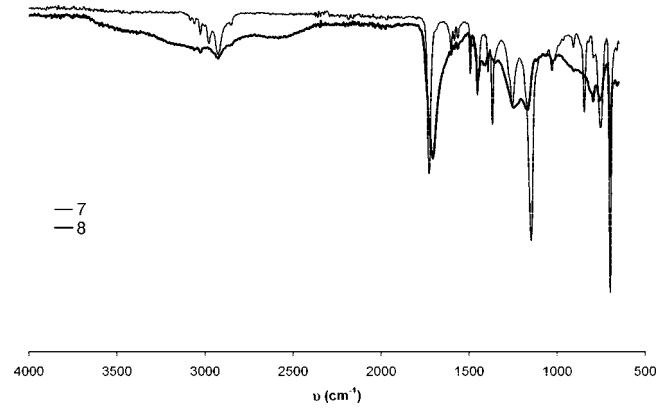

Figure 2. IR spectrum of hydrophobic block copolymers **7** and deprotection product amphiphilic block copolymer, **8**.

Scheme 3[a]

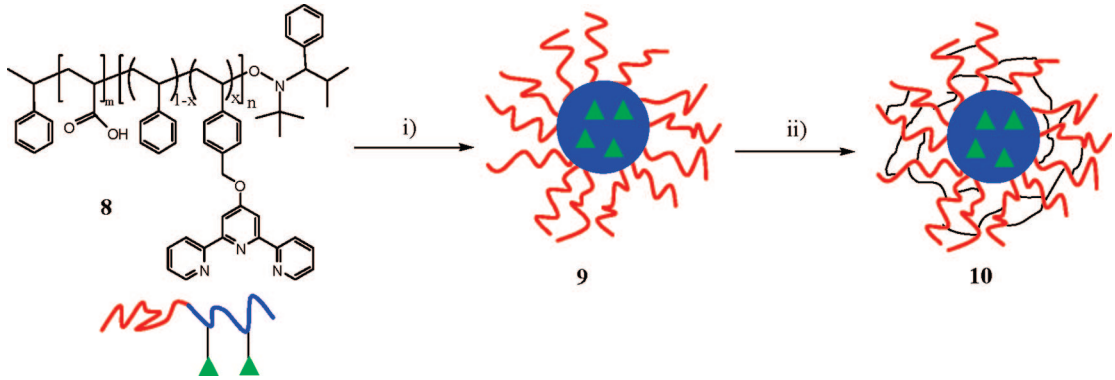

[a] Reagents and conditions: (i) THF, followed by addition of water and dialysis against water; (ii) 2,2′-(ethylenedioxy)bis(ethylamine) (0.25 equiv based upon the acid functionalities) 1-[3′-(dimethylamino)propyl]-3-ethylcarbodiimide methiodide (0.50 equiv to acid functionalities), RT, overnight, followed by dialysis against water.

confirmed by IR and ^{1}H NMR analysis (Figure 2) which highlighted the disappearance of the ester resonances (1726 cm^{-1}) and the appearance of a new broad signal characteristic of a carboxylic acid functionality (1706 cm^{-1}). In addition, further analysis of the IR spectrum highlighted the disappearance of the *tert*-butyl group stretching bands at ca. 1392 and 1367 cm^{-1}. An important aspect of this work was in the retention of the side-chain terpyridine functionality upon ester deprotection given the relatively harsh acidic conditions required to enable this conversion. The retention of the terpyridine functionality in the amphiphilic copolymer, **8**, was confirmed by ^{1}H NMR and IR analysis with the characteristic terpyridine signals (IR: 1601, 1582, 1565 cm^{-1}; ^{1}H NMR: 8.6, 8.0, and 7.6 ppm) evident after deprotection in the same ratio and intensity as observed in **7**.

Self-Assembly of Hydrophobic Core Functionalized Blocks into Micelles and Nanoparticles. Micelles composed of the block copolymer **8** were formed by the slow addition of deionized water (at a rate of about 15 mL/h) to a stirred solution of the polymer at 1 mg/mL in THF.[44] Following extensive dialysis (MWCO ca. 3.5 kDa) of the solution against water, terpyridine core functionalized spherical micelles of narrow size distribution, **9**, were obtained (Scheme 3). The calculated concentration of the micelle solution was determined by measurement of the final volume of micelle obtained together with the initial weight of the polymer precursors used.

The solution of micelles **9** was then cross-linked using amidation chemistry by activating a fraction of the carboxylic acid groups, with 1-[3′-(dimethylamino)propyl]-3-ethylcarbodiimide methiodide followed by reaction with 2,2′-(ethylenedioxy)bis(ethylamine) overnight at ambient temperature (Scheme 3).[15] A theoretical degree of cross-linking of 50% was targeted to ensure accessibility of the reactive functionality within the core domain, yet affording a stable and robust polymeric nanostructure. Previous work has demonstrated that click reactive handles which are embedded within the polystyrene core of a nanoparticle with 50% nominal cross-linking are available to undergo reaction with the complementary click functionality.[81] The terpyridine functionalized nanoparticle, **10**, was then purified by dialysis to remove the urea byproducts and afford a solution of terpyridine core functionalized nanoparticles **10** with a concentration of around 0.32 mg/mL. The presence of the terpyridine functionality within the nanoparticles was difficult to confirm by IR spectroscopy, upon lyophilization of an aliquot, due to the presence of the amide bands upon cross-linking at ca. 1640 and 1560 cm^{-1} which obscured some of the terpyridine signals, although one of the characteristic signal at 1601 cm^{-1} was evident, indicating retention of the terpyridine functionality within the core domain.

Table 2. Characterization Data for Micelles 9 and the Corresponding Nanoparticles 10 and 11

particle	DLS D_h[a] (nm)	TEM D_{av}[b] (nm)	ζ[c] (mV)	DSC T_g[d] (°C)
9	67 ± 3	61 ± 5	−49 ± 1	135, 105
10	58 ± 2	52 ± 4	−21 ± 1	107
11	62 ± 3	58 ± 4	−28 ± 2	n.d.

[a] Number-averaged hydrodynamic diameters in aqueous solution by dynamic light scattering. [b] Average diameters measured by TEM, averaged from the values for ca. 150 particles. [c] Zeta potential, from 12 determinations of 5 runs. [d] Glass transition temperature, taken as the midpoint of the inflection tangent upon the third heating scan.

Zeta potential measurements, which were determined by electrophoretic light scattering (Table 2), were negative and indicated that the surface of the micelles and nanoparticles are negatively charged. As previously reported, the micelle zeta potential value is more negative than that observed for the nanoparticle, which supports the consumption of a portion of the charged carboxylic acid residues upon cross-linking. Successful cross-linking of the micelle was also confirmed by differential scanning calorimetry (DSC) analysis, which confirmed that upon cross-linking throughout the shell layer only a single phase transition corresponding to the polystyrene core was evident compared to the two transitions which were observed in the precursor micelle.

The size, shape, and distribution of these functionalized micelles, **9**, and nanoparticles, **10**, were determined in solution using dynamic light scattering (DLS) and zeta potential measurements and in the solid state (adsorbed) by transmission electron microscopy (TEM) (Figure 3). Significantly, TEM analysis gave nanoparticle and micelle diameters (D_{av}) which were similar to the hydrodynamic diameter (D_h) which was obtained from DLS analysis.

The availability of the terpyridine functionality located within the nanoparticles hydrophobic core domain was determined using solution metal complexation chemistries. Terpyridine is well-known to bind to a range of metals including Ru, Fe, and Cu in a bidentate fashion by reaction of the metal(III) halide precursor as described recently by Schubert and co-workers.[62,65] Initial experiments focused on the incorporation of Ru metal into the nanoparticle cores using established chemistries to afford metal functionalized nanoparticle **11**. This hybrid nanoparticle was characterized using DLS and TEM analysis, and no significant alteration in the size or shape of the nanoparticle upon metal complexation was observed. The incorporation of the Ru metal centers into the hydrophobic core domain was confirmed by UV–vis analysis from the characteristic absorbance which was evident at ca. 390 nm (Figure 4), which can be

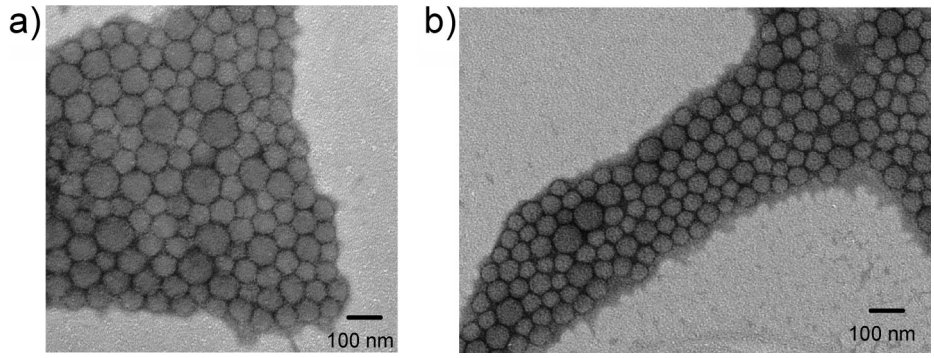

Figure 3. Representative TEM images of (a) micelle **9** and (b) nanoparticle **10**. Samples were stained with phosphotungstic acid, drop-deposited onto a carbon-coated copper grid, and allowed to dry under ambient conditions.

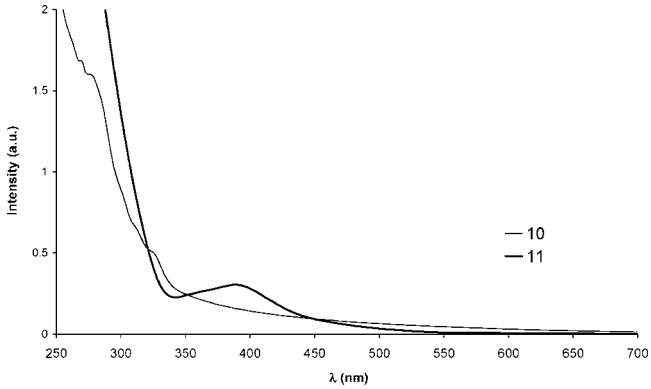

Figure 4. UV–vis absorbance spectrum of **10** and **11** in H_2O at concentrations ca. 0.32 mg/mL.

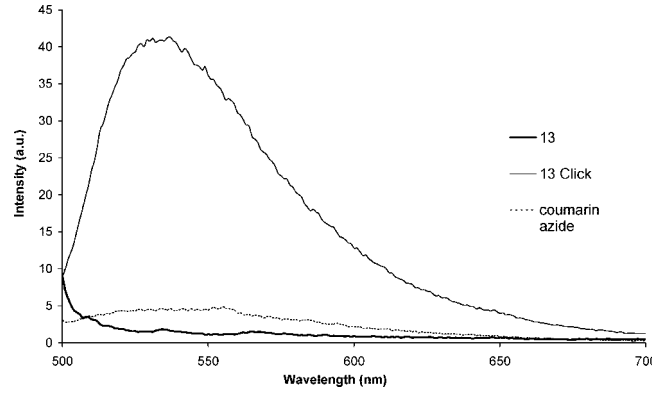

Figure 5. Comparison of the fluorescence emission spectra (excitation wavelength 496 nm) for **12**, coumarin azide, and the "click" reaction of nanoparticle **12**.

attributed to the reported metal–ligand charge transfer (MLCT) band of the mono complexed Ru−terpyridine species.[64] In addition, IR analysis of a lyophilized portion of nanoparticle **11** produced a brown solid which displayed the expected absorbances for the terpyridine monocomplex.

Further experiments explored the complexation of Fe(III) chloride into the nanoparticle scaffold to afford hybrid structure **12**, and this was also found to be successful on the basis of UV–vis (λ_{max} ca. 550 nm) and DLS analysis (55 ± 4 nm); see Experimental Section for further details.[83] Further work is exploring the application of this Fe−terpyridine functional nanoparticle in a range of reactions including the ring opening of epoxides by analogue to the recent work by Lee and co-workers, who utilized a polymer supported mononuclear Fe−terpyridine complex with labile ligands and achieved stereospecific and regioselective products.[84]

One goal of this work was to demonstrate the ability to post-assembly functionalize a nanoparticle to incorporate a reactive or catalytic site within the hydrophobic core domain. This was achieved by adding an organic Cu(I) salt into the terpyridine functionalized domain of the nanoparticle which had been selectively swollen in DMF and then exploring its activity as a 1,3 dipolar cycloaddition "click" catalyst. This reaction was chosen for the initial experiments due to the recent work by Matyjaszewski and co-workers which highlighted that terpyridine ligands in conjunction with Cu(I) salts are active click catalysts, albeit sluggish compared to PMDETA, for the coupling of chain-end azido and alkynyl functionalized polymers.[85] It is proposed that the terpyridine functionality if available throughout the core domain should complex the Cu(I) salt to form an in-situ active click catalyst. To test whether an active catalyst was formed, we utilized a previously reported methodology which employs a fluorogenic reaction between an azido coumarin and an alkynyl small molecule. This technique has been demonstrated by Wang and co-workers[78] as well as Wooley and Hawker[52] to be an effective tool for the confirmation of a cycloaddition reaction due to the triggering of fluorescence upon changing the coumarin's electronic structure when it undergoes cycloaddition to convert its azido functionality into a triazole moiety. Thus, this methodology provides us with a readily available external response (fluorescence) which can be monitored to determine whether the Cu(I) complex forms and is successful in mediating the "click" reaction.

Experimentally, the core of the nanoparticle was first swollen by dialysis into a mixed DMF:water solvent system (1:10 v/v) followed by addition of a Cu(I) source and stirring for 1 h. The resultant solution, **13**, was analyzed by UV–vis spectroscopy, and a shoulder was observed at 330 nm, which indicated that a terpyridine−Cu(I) complex had formed within the nanoparticle core domain.[63] To confirm whether this Cu−terpyridine complex was active in click catalysis, phenylethynyl and 3-azidocoumarin were added with stirring, and the solution was allowed to react at room temperature for 4 h. After this time an aliquot was removed and analyzed using fluorescence spectroscopy, and a characteristic emission for the fluorogenic coumarin was observed at ca. 550 nm (Figure 5). Two control reactions were performed: the first in which nanoparticle **10** was treated under identical conditions with the azido-coumarin and alkynyl but without the presence of the Cu(I) species and this case no fluorescence was observed and the second in which the Cu(I) and reagents were allow to react in the presence of a nanoparticle which did not contain terpyridine functionality. This initial result indicates that the terpyridine functionality embedded within the nanoparticle is indeed available for both complexation and subsequent mediation of catalysis reactions. The Cu−terpyridine complex formed in this work within the nanoparticle core has been demonstrated to be active in the "click" reaction of simple

small molecules. Further work is currently underway to further explore the catalytic activity of these metal functionalized nanoparticles in a range of reactions.

Conclusions

In this work we have reported the copolymerization of a terpyridine functionalized styrene monomer with styrene using NMP techniques. This route enables access to moderate loadings of functional monomer into the polymer although some loss of polymerization control is observed at monomer loadings above 5%. Using these polymerization data, an acrylate−styrene diblock was targeted with selective incorporation of around 6% terpyridine functionality relative to the nonfunctionalized styrene segment. This block could then be converted to its amphiphilic derivative using established deprotection chemistries with no loss in terpyridine functionality evident by ^{1}H NMR and IR analysis. This amphiphile was then selectively assembled into spherical micelles and cross-linked throughout a portion of the carboxylic acid residues in the shell layer. This afforded a well-defined robust nanoparticle in which the core domain contained a targeted degree of terpyridine functionality. This functionality was then utilized to complex metal centers into the core domain of the particle. Initial results confirm that this functionality is available, and by careful choice of the metal center a catalytically active nanoparticle can be prepared. Further work is currently focusing on the utilization of this nanoparticle scaffold for the selective complexation of other metal salts and the application of these systems as novel functional materials.

Acknowledgment. This work is based on research supported by the Royal Society (Dorothy Hodgkin Research Fellowship to R.K.O'R), Downing College, EPSRC, IRC in Nanotechnology, Nuffield Foundation, and the Department of Chemistry. Dr. Jeremy Skepper (University of Cambridge) is thanked for assistance with TEM imaging.

References and Notes

(1) Hawker, C. J.; Bosman, A. W.; Harth, E. *Chem. Rev.* **2001**, *101*, 3661–3688.
(2) Kamigaito, M.; Ando, T.; Sawamoto, M. *Chem. Rev.* **2001**, *101*, 3689–3745.
(3) Matyjaszewski, K.; Xia, J. H. *Chem. Rev.* **2001**, *101*, 2921–2990.
(4) Perrier, S.; Takolpuckdee, P. *J. Polym. Sci., Part A: Polym. Chem.* **2005**, *43*, 5347–5393.
(5) Chiefari, J.; Chong, Y. K.; Ercole, F.; Krstina, J.; Jeffery, J.; Le, T. P. T.; Mayadunne, R. T. A.; Meijs, G. F.; Moad, C. L.; Moad, G.; Rizzardo, E.; Thang, S. H. *Macromolecules* **1998**, *31*, 5559–5562.
(6) Mayadunne, R. T. A.; Rizzardo, E.; Chiefari, J.; Chong, Y. K.; Moad, G.; Thang, S. H. *Macromolecules* **1999**, *32*, 6977–6980.
(7) Georges, M. K.; Veregin, R. P. N.; Kazmaier, P. M.; Hamer, G. K. *Macromolecules* **1993**, *26*, 2987–2988.
(8) Isrealachvilli, J. N.; Mitchell, D. J.; Ninham, B. W. *J. Chem. Soc., Faraday Trans.* **1976**, *72*, 1525–1569.
(9) Klok, H. A.; Lecommandoux, S. *Adv. Mater.* **2001**, *13*, 1217–1229.
(10) Lowik, D. W. P. M.; van Hest, J. C. M. *Chem. Soc. Rev.* **2004**, *33*, 234–245.
(11) Cao, L.; Manners, I.; Winnik, M. A. *Macromolecules* **2001**, *34*, 3353–3360.
(12) Sanji, T.; Nakatsuka, Y.; Kitayama, F.; Sakurai, H. *Chem. Commun.* **1999**, 2201–2202.
(13) Huang, H. Y.; Remsen, E. E.; Wooley, K. L. *Chem. Commun.* **1998**, 1415–1416.
(14) Butun, V.; Billingham, N. C.; Armes, S. P. *J. Am. Chem. Soc.* **1998**, *120*, 12135–12136.
(15) Thurmond, K. B.; Kowalewski, T.; Wooley, K. L. *J. Am. Chem. Soc.* **1997**, *119*, 6656–6665.
(16) Ding, J. F.; Liu, G. J. *Macromolecules* **1998**, *31*, 6554–6558.
(17) Chen, Z.; Cui, H.; Hales, K.; Li, Z.; Qi, K.; Pochan, D. J.; Wooley, K. L. *J. Am. Chem. Soc.* **2005**, *127*, 8592–8593.
(18) Hamley, I. W.; Ansari, I. A.; Castelletto, V.; Nuhn, H.; Roesler, A.; Klok, H.-A. *Biomacromolecules* **2005**, *6*, 1310–1315.
(19) Cornelissen, J. J. L. M.; Fischer, M.; Sommerdijk, N. A. J. M.; Nolte, R. J. M. *Science* **1998**, *280*, 1427–1430.
(20) Minich, E. A. *Polymer* **2004**, *45*, 1951–1957.
(21) Hanley, K. J.; Lodge, T. P.; Huang, C. I. *Macromolecules* **2000**, *33*, 5918–5931.
(22) Li, Z.; Chen, Z.; Cui, H.; Hales, K.; Wooley, K. L.; Pochan, D. J. *Langmuir* **2007**, *23*, 4689–4694.
(23) Hou, S.; Man, K. Y. K.; Chan, W. K. *Langmuir* **2003**, *19*, 2485–2490.
(24) Guler, M. O.; Pokorski, J. K.; Appella, D. H.; Stupp, S. I. *Bioconjugate Chem.* **2005**, *16*, 501–503.
(25) Liu, D.; De Feyter, S.; Cotlet, M.; Wiesler, U.-M.; Weil, T.; Herrmann, A.; Muellen, K.; De Schryver, F. C. *Macromolecules* **2003**, *36*, 8489–8498.
(26) Zhang, L. F.; Eisenberg, A. *Science* **1995**, *268*, 1728–1731.
(27) Choucair, A.; Lavigueur, C.; Eisenberg, A. *Langmuir* **2004**, *20*, 3894–3900.
(28) Terreau, O.; Luo, L. B.; Eisenberg, A. *Langmuir* **2003**, *19*, 5601–5607.
(29) Reiss, G. *Prog. Polym. Sci.* **2003**, *28*, 1107–1170.
(30) Raez, S.; Manners, I.; Winnik, M. A. *J. Am. Chem. Soc.* **2002**, *124*, 10381–10395.
(31) Wooley, K. L. *J. Polym. Sci., Part A: Polym. Chem.* **2000**, *38*, 1397–1407.
(32) Vriezema, D. M.; Aragones, M. C.; Elemans, J. A. A. W.; Cornelissen, J. J. L. M.; Rowan, A. E.; Nolte, R. J. M. *Chem. Rev.* **2005**, *105*, 1445–1489.
(33) Rosler, A.; Vandermeulen, G. W. M.; Klok, H. A. *Adv. Drug Delivery Rev.* **2001**, *53*, 95–108.
(34) Torchilin, V. P. *Cell. Mol. Life Sci.* **2004**, *61*, 2549–2559.
(35) Pressly, E. D.; Rossin, R.; Hagooly, A.; Fukukawa, K.; Messmore, B. W.; Welch, M. J.; Wooley, K. L.; Lamm, M. S.; Hule, R. A.; Pochan, D. J.; Hawker, C. J. *Biomacromolecules* **2007**, *8*, 3126–3134.
(36) Read, E. S.; Armes, S. P. *Chem. Commun.* **2007**, 3021–3035.
(37) O'Reilly, R. K.; Hawker, C. J.; Wooley, K. L. *Chem. Soc. Rev.* **2006**, *35*, 1068–1083.
(38) Hawker, C. J.; Wooley, K. L. *Science* **2005**, *309*, 1200–1205.
(39) Elemans, J. A. A. W.; Rowan, A. E.; Nolte, R. J. M. *J. Mater. Chem.* **2003**, *13*, 2661–2670.
(40) Prochaska, K.; Baloch, M. K. *Makromol. Chem.* **1979**, *180*, 2521–2523.
(41) Guo, A.; Liu, G. J.; Tao, J. *Macromolecules* **1996**, *29*, 2487–2493.
(42) Henselwood, F.; Liu, G. J. *Macromolecules* **1997**, *30*, 488–493.
(43) Sumerlin, B. S.; Lowe, A. B.; Thomas, D. B.; Convertine, A. J.; Donovan, M. S.; McCormick, C. L. *J. Polym. Sci., Part A: Polym. Chem.* **2004**, *42*, 1724–1734.
(44) Huang, H. Y.; Kowalewski, T.; Remsen, E. E.; Gertzmann, R.; Wooley, K. L. *J. Am. Chem. Soc.* **1997**, *119*, 11653–11659.
(45) Thurmond, K. B.; Kowalewski, T.; Wooley, K. L. *J. Am. Chem. Soc.* **1996**, *118*, 7239–7240.
(46) Liu, S.; Armes, S. P. *J. Am. Chem. Soc.* **2001**, *123*, 9910–9911.
(47) Iijima, M.; Nagasaki, Y.; Okada, T.; Kato, M.; Kataoka, K. *Macromolecules* **1999**, *32*, 1140–1146.
(48) Zhang, L.; Katapodi, K.; Davies, T. P.; Barner-Kowollik, C.; Stenzel, M. H. *J. Polym. Sci., Part A: Polym. Chem.* **2006**, *44*, 2177–2194.
(49) Joralemon, M. J.; O'Reilly, R. K.; Hawker, C. J.; Wooley, K. L. *J. Am. Chem. Soc.* **2005**, *127*, 16892–16899.
(50) Ma, Q.; Remsen, E. E.; Kowalewski, T.; Schaefer, J.; Wooley, K. L. *Nano Lett.* **2001**, *1*, 651–655.
(51) Murthy, K. S.; Ma, Q.; Clark, C. G., Jr.; Remsen, E. E.; Wooley, K. L. *Chem. Commun.* **2001**, 773–774.
(52) O'Reilly, R. K.; Joralemon, M. J.; Hawker, C. J.; Wooley, K. L. *Eur. J. Chem.* **2006**, *12*, 6776–6786.
(53) Butun, V.; Wang, X. S.; Banez, M. V. D.; Robinson, K. L.; Billingham, N. C.; Armes, S. P.; Tuzar, Z. *Macromolecules* **2000**, *33*, 1–3.
(54) O'Reilly, R. K. *Philos. Trans. R. Soc. London, A* **2007**, *365*, 2863–2878.
(55) Dwars, T.; Paetzold, E.; Oehme, G. *Angew. Chem., Int. Ed.* **2005**, *44*, 7174–7199.
(56) Kobayashi, S.; Akiyama, R. *Chem. Commun.* **2003**, 449–460.
(57) Mason, B. P.; Bogdan, A. R.; Goswami, A.; McQuade, D. T. *Org. Lett.* **2007**, *9*, 3449–3451.
(58) Schubert, U. S.; Eschbaumer, C.; Hien, O.; Andres, P. R. *Tetrahedron Lett.* **2001**, *42*, 4705–4707.
(59) Hofmeier, H.; Schubert, U. S. *Chem. Soc. Rev.* **2004**, *33*, 373–399.
(60) Lohmeijer, B. G. G.; Schubert, U. S. *J. Polym. Sci., Part A: Polym. Chem.* **2004**, *42*, 4016–4027.
(61) Schubert, U. S.; Hofmeier, H. *Macromol. Chem. Phys.* **2002**, *203*, 561–566.
(62) Chiper, M.; Meier, M. A. R.; Kranenburg, J. M.; Schubert, U. S. *Macromol. Chem. Phys.* **2007**, *208*, 679–689.
(63) Lohmeijer, B. G. G.; Schubert, U. S. *Macromol. Chem. Phys.* **2003**, *204*, 1072–1078.

(64) Lohmeijer, B. G. G.; Schlaad, H.; Schubert, U. S. *Macromol. Symp.* **2003**, *196*, 125–135.
(65) Lohmeijer, B. G. G.; Schubert, U. S. *J. Polym. Sci., Part A: Polym. Chem.* **2003**, *41*, 1413–1427.
(66) Gohy, J. F.; Hofmeier, H.; Alexeev, A.; Schubert, U. S. *Macromol. Chem. Phys.* **2003**, *204*, 1524–1530.
(67) Andres, P. R.; Schubert, U. S. *Adv. Mater.* **2004**, *16*, 1043–1068.
(68) Calzia, K. J.; Tew, G. N. *Macromolecules* **2002**, *35*, 6090–6093.
(69) Tew, G. N.; Aamer, A. K.; Shunmuugam, R. *Polymer* **2005**, *46*, 8440–8447.
(70) Shunmuugam, R.; Tew, G. *J. Am. Chem. Soc.* **2005**, *127*, 13567–13572.
(71) Aamer, A. K.; Tew, G. N. *Macromolecules* **2007**, *40*, 2737–2744.
(72) Rostovtsev, V. V.; Green, L. G.; Fokin, V. V.; Sharpless, K. B. *Angew. Chem., Int. Ed.* **2002**, *41*, 2596–2599.
(73) Kolb, H. C.; Finn, M. G.; Sharpless, K. B. *Angew. Chem., Int. Ed.* **2001**, *40*, 2004–2021.
(74) Binder, W. H.; Sachsenhofer, R. *Macromol. Chem. Phys.* **2007**, *208*, 15–54.
(75) Benoit, D.; Chaplinski, V.; Braslau, R.; Hawker, C. J. *J. Am. Chem. Soc.* **1999**, *121*, 3904–3920.
(76) Schubert, U. S.; Schmatloch, S.; Precup, A. A. *Des. Monomers Polym.* **2002**, *5*, 211–221.
(77) Gujadhur, R.;Venkataraman, D.;Kintigh, J. T. *Tetrahedron Lett*. **2001**, *42*, 4971–4973.
(78) Sivakumar, K.; Xie, F.; Cash, B. M.; Long, S.; Barnhill, H. N.; Wang, Q. *Org. Lett.* **2004**, *6*, 4603–4606.
(79) Andres, P. R.; Hofmeier, H.; Lohmeijer, B. G. G.; Schubert, U. S. *Synthesis* **2003**, *18*, 2865–2871.
(80) Ma, Q.; Wooley, K. L. *J. Polym. Sci., Part A: Polym. Chem.* **2000**, *38*, 4805–4820.
(81) O'Reilly, R. K.; Joralemon, M. J.; Hawker, C. J.; Wooley, K. L. *Chem. Mater.* **2005**, *17*, 5976–5988.
(82) Deleted in proof.
(83) Hofmeier, H.; Schubert, U. S. *Macromol. Chem. Phys.* **2003**, *204*, 1391–1397.
(84) Yoo, D.-W.; Yoo, S.-K.; Kim, C.; Lee, J.-K. *Chem. Commun.* **2002**, 3931–3932.
(85) Golas, P. L.; Tsarevsky, N. V.; Sumerlin, B. S.; Matyjaszewski, K. *Macromolecules* **2006**, *39*, 6451–6457.

MA702702J